

Generalized Beltrami flow — a model of thin-disk and narrow-jet system

Z. Yoshida¹ and N. L. Shatashvili^{2,3}

¹Graduate School of Frontier Sciences, The University of Tokyo, Chiba 277-8561, Japan

²Faculty of Exact and Natural Sciences, Javakishvili Tbilisi State University, Tbilisi 0128, Georgia

³Andronikashvili Institute of Physics, Javakishvili Tbilisi State University, Tbilisi 0177, Georgia

Abstract. In the vicinity of a massive object of various scales (ranging from young stars to galactic nuclei), mass flow creates a spectacular structure combining a thin disk and collimated jet. Despite a wide range of scaling parameters (such as Reynolds number, Lundquist number, ionization fractions, Lorentz factor, etc.), they exhibit a remarkable similarity that must be dictated by a universal principle. A generalized Beltrami condition has been formulated as a succinct representation of such a principle. The singularity at the center of the Keplerian rotation forces the flow to align with the “generalized vorticity” (including the effect of localized density and finite dissipation) which appears as an axle penetrating the disk, i.e. the jet is a Beltrami flow. Based on the Beltrami flow model, an analytical expression of a disk-jet system has been constructed by the method of similarity solution.

1. Introduction

The combination of a thin disk and collimated jet is a common structure that is created in the vicinity of a massive object [2, 1, 12, 6, 13]. Beneath a large variety of scales, constituents, and local processes of such systems, there must be a simple and universal principle that dictates the remarkably similar geometry; see Fig. 1. Here we show that the collimated structure of jet is a natural consequence of the *alignment* of the flow velocity and the vorticity, i.e. so-called *Beltrami condition* determines the structure. On a Keplerian thin disk, the vorticity becomes a vertical vector with a magnitude $\propto r^{-3/2}$ (r is the radius from the center of the disk), which appears as a spindle of the disk. Then, the alignment is the unique solution for avoiding singularity of Coriolis force near the center. However, we need to generalize the “vorticity” to deal with the strong heterogeneity of the disk-jet system, as well as to account for the dissipation that causes accretion. The mission of this study is to formulate an appropriate *generalized vorticity* to which the disk-jet flow aligns.

Let us start by a short review of the Beltrami vector field which has wide applications as a model of various *vortex structures* found in nature. The Beltrami condition, demanding the alignment of flow and its vorticity, forces the total *energy density* (consisting of thermal energy, kinetic energy, and other energies of coupled fields such as gravitational or electromagnetic) to distribute homogeneously (so called Bernoulli condition); the Beltrami-Bernoulli condition, thus, fits the notion of “relaxed state.” While a Beltrami field was discovered by many researchers as a particular type of equilibrium state [4, 14], or *free decay* solution [10], in fluids or plasmas, its relation to the *helicity* was noticed in the study of “force-free magnetic fields” in plasmas; Woltjer [27] invoked the helicity as a constraint in minimizing the magnetic energy; Taylor [25] considered that the “relaxed state” is the energy minimizer under the lugged constancy of the total helicity; the corresponding Euler-Lagrange equation becomes the eigenvalue problem of the curl operator; see [29] for the mathematical characterization of the curl operator and its eigenfunctions. We can actually observe Taylor relaxed states on various experiments [26], as well as in some astronomical systems; e.g. [8, 11]. The helicity constraint causes a finite *vorticity* in the relaxed state, resulting in interesting topological properties of field-lines [17]. In the context of Hamiltonian mechanics, the helicity is regarded as a Casimir element representing the defect of the governing symplectic geometry [18]; a Beltrami field is an equilibrium point on a *helicity leaf*.

The Beltrami fields constitute an interesting, widely-applied class of vectors (or axial vectors) with “twisted” field-lines; e.g. [3, 5, 24]. Not only for describing equilibrium states, they are applied to analyze waves [30, 7], instabilities [31], and turbulence [20, 9, 28] (here we can cite only a short list of references).

A variety of generalizations have been proposed. Including the cross helicity as an additional constraint, we obtain a flow parallel to the magnetic field and the resultant hydrodynamic pressure balancing with a static pressure [23]. The two-fluid (Hall MHD) formulation elucidates a fundamental structure in the coupling of flow and magnetic field in terms of the *canonical vorticities* [15]; the simultaneous ion and electron Beltrami conditions yields the *double Beltrami fields*, which have various applications in both laboratory and astrophysical plasmas; e.g. [19, 16, 32]. Another generalization is made by including the coupling of vortex and compressible motions; by boosting such generalized Beltrami fields, we obtain modulating nonlinear Alfvén waves [33].

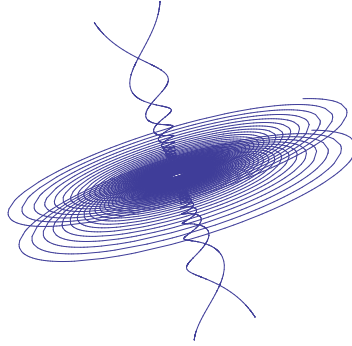


Figure 1. In a disk-jet system, the accreting flow and jet align parallel to a *generalized vorticity*. This figure shows the streamlines of a “generalized Beltrami flow” to be constructed in Sec. 5

This work extends the scope of Beltrami fields to show that the disk-jet system is a “generalized” Beltrami vortex [21]; the generalization is made by introducing a new *generalized vorticity* that combines the vorticity of a “reduced momentum” —the reduction is to account for a viscous dissipation as well as to subtract the centrifugal force of the Keplerian rotation.

2. Generalized vorticity and Beltrami condition

To demonstrate how the alignment condition arises and how it determines the structure of a thin disk and narrowly-collimated jet, we invoke a simple model of neutral fluid; for a generalization to magneto-fluid, see Appendix A. Let $\mathbf{P} = \rho\mathbf{V}$ denote the mechanical momentum density, where ρ is the mass density and \mathbf{V} is the (ion) flow velocity. The momentum equation read as

$$\partial_t \mathbf{P} + \nabla \cdot (\mathbf{V}\mathbf{P}) = -\rho\nabla\phi - \nabla p - \nabla \cdot \mathbf{\Pi}, \quad (1)$$

where ϕ is the gravity potential, p is the scalar pressures, and $\mathbf{\Pi}$ is the (effective) viscosity tensor. The variables are normalized as follows: We choose a representative flow velocity V_0 and a mass density ρ_0 in the disk, and normalize \mathbf{V} and ρ by these units. The energy densities $\rho\phi$ (gravitational) and p (thermal) are normalized by the unit kinetic energy density $\mathcal{E}_0 := \rho_0 V_0^2/2$. The independent variables (coordinate \mathbf{x} and time t) are normalized by the system size L_0 and the corresponding transit time $T_0 = L_0/V_0$.

We consider stationary solutions; putting $\partial_t = 0$ in (1), we obtain

$$\nabla \cdot (\mathbf{V}\mathbf{P}) = -\rho\nabla\phi - \nabla p - \nabla \cdot \mathbf{\Pi}. \quad (2)$$

In order to derive a term that balances with the viscosity term, we decompose the “inertia term” [the left-hand side of (2)] as follows: we first write

$$\rho = \rho_1 \rho_2, \quad (3)$$

and denote

$$\mathbf{P}_1 := \rho_1 \mathbf{V}, \quad \mathbf{P}_2 := \rho_2 \mathbf{V}. \quad (4)$$

Using these variables, we may write

$$\nabla \cdot (\mathbf{V}\mathbf{P}) = \nabla \cdot (\rho \mathbf{V}\mathbf{V}) = (\nabla \cdot \mathbf{P}_1)\mathbf{P}_2 + (\mathbf{P}_1 \cdot \nabla)\mathbf{P}_2. \quad (5)$$

In the conventional formulation of fluid mechanics, we choose $\rho_2 = 1$ and $\rho_1 = \rho$. Then, using the mass conservation law $\partial_t \rho + \nabla \cdot \mathbf{P} = 0$, we can rewrite the left-hand side of (1) as $\rho[\partial_t \mathbf{V} + (\mathbf{V} \cdot \nabla)\mathbf{V}]$. In the preset analysis, however, we choose a different separation of the inertia term in order to match $(\nabla \cdot \mathbf{P}_1)\mathbf{P}_2$ with the viscosity term. By a reduced $\rho_2 (< 1)$, we will define a *generalized vorticity* of a *reduced momentum*. Multiplying (ρ_2/ρ_1) on both sides of (2), we obtain (assuming a barotropic relation, we put $\nabla p = \rho \nabla h$ with an enthalpy h)

$$\mathbf{P}_2 \times \boldsymbol{\Omega}_2 = \frac{1}{2} \nabla P_2^2 + \rho_2^2 \nabla(\phi + h) + \frac{\rho_2}{\rho_1} [(\nabla \cdot \mathbf{P}_1)\mathbf{P}_2 + \nabla \cdot \boldsymbol{\Pi}], \quad (6)$$

where

$$\boldsymbol{\Omega}_2 := \nabla \times \mathbf{P}_2 \quad (7)$$

is a *generalized vorticity*.

In the next section, we will show that a generalized Beltrami condition, demanding that $\boldsymbol{\Omega}_2$ parallels \mathbf{P}_2 (thus, (6) holds with both sides being zero), is a unique recourse to avoid singular energy densities in a disk-jet geometry.

3. Beltrami Model of Disk-Jet System

Now we consider an axisymmetric ($\partial_\theta = 0$ in the r - θ - z coordinates) disk-jet system. A massive central object produces $\phi = -MG/r$ (we neglect the mass in the disk and jet). In the disk, $\mathbf{V} \approx V_\theta \mathbf{e}_\theta$ with the Keplerian velocity $V_\theta \propto r^{-1/2}$. Then, $\nabla \times \mathbf{V} \propto r^{-3/2} \mathbf{e}_z$. The momentum is strongly localized in the thin disk, and the vorticity diverges near the axis. This particular configuration poses strong constraints on the force balance equation (6), allowing only a special class of solutions to exist; following conclusions are readily deducible.

3.1. Balance of viscosity force and partial inertia

In the disk, a radial flow (much smaller than V_θ) is caused by the viscosity (a finite dissipation breaks the conservation of the angular momentum and enables the flow to cause accretion).

Since the flow \mathbf{V} is primarily in the azimuthal (θ) direction, the viscosity force can be approximated as (under assumption of the azimuthal symmetry, $\nabla \cdot \mathbf{V} \approx 0$)

$$-\nabla \cdot \boldsymbol{\Pi} \approx -\nabla \times (\rho \eta \nabla \times \mathbf{V}), \quad (8)$$

where η is the shear viscosity coefficient. In a Keplerian thin disk, where $\mathbf{V} \approx V_\theta r^{-1/2} \mathbf{e}_\theta$, and $\nabla(\rho \eta)$ is approximately vertical, we may estimate

$$-\nabla \cdot \boldsymbol{\Pi} \approx -\rho \eta \nabla \times (\nabla \times \mathbf{V}) = -\rho \eta V_\theta \frac{3}{4} r^{-5/2} \mathbf{e}_\theta. \quad (9)$$

Hence, we may write $-\nabla \cdot \boldsymbol{\Pi} = -\nu \mathbf{P}$ with a positive coefficient $\nu(r)$, i.e., the viscosity force is primarily in the azimuthal (toroidal) direction, which can be balanced by the

term $(\rho_2/\rho_1)(\nabla \cdot \mathbf{P}_1)\mathbf{P}_2$ that has been extracted from the inertia term; see (5). Using the steady-state mass conservation law $\nabla \cdot \mathbf{P} = 0$, we observe

$$\rho_1^{-1} \nabla \cdot \mathbf{P}_1 = \rho_2 \mathbf{V} \cdot \nabla \rho_2^{-1} = -\mathbf{V} \cdot \nabla \log \rho_2.$$

Hence, the balance of the viscosity and the partial inertia term demands

$$\mathbf{V} \cdot \nabla \log \rho_2 = \nu, \quad (10)$$

which determines the parameter ρ_2 . (Since $\partial_\theta = 0$, we can integrate (10) for ρ_2 along the streamline of \mathbf{V} on the poloidal r - z plane.)

The remaining part ρ_1 of the density is determined by the mass conservation law: By $\nabla \cdot \mathbf{P} = \nabla \cdot (\rho \mathbf{V}) = \rho_2 \mathbf{V} \cdot \nabla \rho_1 + \rho_1 \mathbf{V} \cdot \nabla \rho_2 + \rho_1 \rho_2 \nabla \cdot \mathbf{V} = 0$ and (10), we obtain a relation

$$\mathbf{V} \cdot \nabla \log \rho_1 = -\nabla \cdot \mathbf{V} - \nu. \quad (11)$$

3.2. Beltrami condition

Near the axis, the poloidal component of the flow begins to have an appreciable vertical (z) component —this is the place where the jet is created; we are going to unearth the mechanism that collimates the flow.

After balancing the third and fourth terms in (6), the remaining terms do not have a toroidal (azimuthal) component. In fact, the right-hand-side gradient terms have only poloidal components, and hence, the left-hand-side $\mathbf{P}_2 \times \boldsymbol{\Omega}_2$ must not have a toroidal component (to put it in another way, we have extracted the partial inertia term $-(\rho_2/\rho_1)(\nabla \cdot \mathbf{P}_1)\mathbf{P}_2$ from the total inertia to separate the toroidal component). The vorticity $\boldsymbol{\Omega}_2$ includes a singular factor $\nabla \times \mathbf{V} \propto r^{-3/2} \mathbf{e}_z$. To eliminate the divergence of $\mathbf{P}_2 \times \boldsymbol{\Omega}_2$ near the axis, \mathbf{P}_2 must align to $\boldsymbol{\Omega}_2$, i.e., the *Beltrami condition*

$$\boldsymbol{\Omega}_2 = \lambda \mathbf{P}_2 \quad (12)$$

must be satisfied, where λ is a certain scalar function. The flow $\mathbf{V} = \mathbf{P}_2/\rho_2$ is, therefore, collimated by the *generalized vorticity* $\boldsymbol{\Omega}_2$ creating a jet.

Remark 1 Here the essential part of the Beltrami condition is its poloidal component, which dictates the poloidal flow so as to eliminate the toroidal component of the inertia term $\mathbf{P}_2 \times \boldsymbol{\Omega}_2$. As for the toroidal flow $V_\theta \mathbf{e}_\theta$, which yields primarily a radial (centrifugal) inertia force, the “Beltrami condition” brings about an extra constraint. In fact, if we were to use the conventional vorticity $\boldsymbol{\Omega} = \nabla \times \mathbf{V}$ (i.e., if $\rho_2 = 1$) and estimate the centrifugal force of the Keplerian flow $\mathbf{V} = V_0 r^{-1/2} \mathbf{e}_\theta$, the term $\mathbf{P} \times \boldsymbol{\Omega}$ contributes a half of the total centrifugal force $(\mathbf{V} \cdot \nabla) \mathbf{P} = \rho V_0^2 / r$, while the term $\nabla V^2 / 2$ on the right-hand side of (6) contributes the remaining half; combining these two terms, we obtain the right balance with the gravity $-\rho M G / r^2$. Hence, the conventional Beltrami condition $\mathbf{P} \times \boldsymbol{\Omega} = 0$ would lead to an inadequate estimate of the toroidal flow. However, our generalized Beltrami condition, based on the generalized vorticity $\boldsymbol{\Omega}_2$ (including $\rho_2 \neq 1$), can be made consistent with the Keplerian velocity; see Sec. 5.

3.3. Bernoulli condition

When the Beltrami condition eliminates the left-hand side of (6), the remaining potential forces must balance to achieve the *Bernoulli condition* [15] that reads as

$$\frac{1}{2\rho_2^2} \nabla P_2^2 + \nabla(\phi + h) = \nabla \left(\frac{1}{2} V^2 + \phi + h \right) + V^2 \nabla \log \rho_2 = 0. \quad (13)$$

The system of determining equations is summarized as follows: By (10), we determine ρ_2 for a given ν . This equation involves $\mathbf{V} = \mathbf{P}/\rho$ that is governed by the Beltrami equation (12). After determining \mathbf{V} and ρ_2 , we can solve the Bernoulli equation (13) to determine h (the gravitational potential is approximated by $\phi = -MG/r$).

4. Parameterization by Clebsch potential

We may rewrite the determining equations (10)-(13) in a succinct form by invoking the Clebsch parameterization. In an axisymmetric geometry, the divergence-free vector \mathbf{P} may be parameterized as

$$\mathbf{P} = \nabla\psi \times \nabla\theta + I\nabla\theta, \quad (14)$$

where $I = \rho r V_\theta$. Both ψ and I do not depend on θ . Since $\mathbf{P} \cdot \nabla\psi = 0$, the level sets (contours) of ψ are the streamlines of \mathbf{P} (or those of $\mathbf{V} = \mathbf{P}/\rho$). In a disk region, $rV_\theta \propto r^{1/2}$, while ρ is a strongly localized function with respect to z .

Substituting (14) into (10) yields

$$\nu = \frac{1}{\rho} \mathbf{P} \cdot \nabla \log \rho_2 = \frac{1}{r\rho} \{\log \rho_2, \psi\}, \quad (15)$$

where $\{a, b\} := (\partial_r b)(\partial_z a) - (\partial_r a)(\partial_z b)$. For a given set of \mathbf{P} , ρ and ν , we can solve (15) to determine ρ_2 , as well as $\rho_1 = \rho/\rho_2$ that is consistent to (11).

Substituting (14) into the Beltrami condition (12), we obtain, from the toroidal component,

$$\lambda \rho_1^{-1} \nabla\psi = \nabla(\rho_1^{-1} I), \quad (16)$$

implying that $\rho_1^{-1} I =: I_2 = I_2(\psi)$ and $\lambda \rho_1^{-1} = I_2'(\psi)$ (we denote $f'(\psi) = df(\psi)/d\psi$), and, from the poloidal component,

$$\mathcal{L}\psi - \nabla\psi \cdot \nabla \log \rho_1 = -\rho_1^2 I_2'(\psi) I_2(\psi), \quad (17)$$

where $\mathcal{L}\psi := r\partial_r(r^{-1}\partial_r\psi) + \partial_z^2\psi$. This elliptic partial differential equation determines the poloidal-momentum Clebsch potential ψ .

The Beltrami condition has decoupled the gradient forces from the momentum equation, which must balance separately—the Bernoulli condition (13) which now reads as the determining equation of the enthalpy:

$$\nabla h = -\nabla \left[\frac{1}{2r^2\rho^2} (|\psi|^2 + I^2) + \phi \right] - \frac{1}{r^2\rho^2} (|\psi|^2 + I^2) \nabla \log \rho_2. \quad (18)$$

5. Analytic Similarity Solution

5.1. A similarity solution modeling disk-jet structure

In this section, we construct a *similarity solution* of the model (17), which describes a fundamental disk-jet structure. We define

$$\tau := \frac{z}{r} \quad (r > 0), \quad (19)$$

and an orthogonal variable ($\nabla\tau \cdot \nabla\sigma = 0$)

$$\sigma := \sqrt{r^2 + z^2}. \quad (20)$$

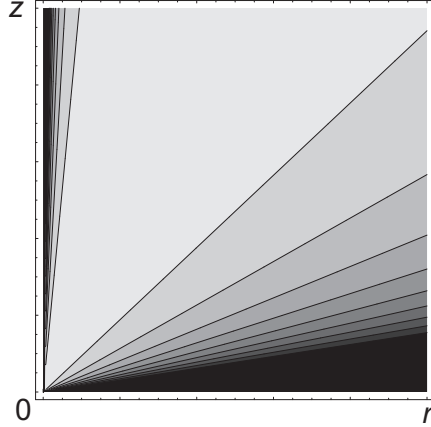


Figure 2. The momentum field (contours of ψ that describe the streamlines of the poloidal component of \mathbf{P}) of the similarity solution (with $D = 1$, $p = 1$, $J = 0.1$ and $q = 1$).

In the thin disk region, we may approximate $\sigma \sim r$, while in the narrow jet region, $\sigma \sim z$. The system is mirror symmetry with respect to the $z = 0$ plane, and the axes $r = 0$ and $z = 0$ are left as singularities. We consider ψ such that

$$\psi = \psi(\tau) = -J\tau^p - D\tau^{-q}, \quad (21)$$

where J and p (D and q) are positive constants, which control the strength of the jet (disk) flow.

As shown in Fig. 2, this ψ models a disk-jet flow. The level sets of ψ (hence, those of τ) are the streamlines of \mathbf{P} . On the other hand, σ serves as the coordinate directed parallel to the streamlines. We assume that ρ_1 is written as

$$\rho_1(\tau, \sigma) = \rho_{\perp}(\tau)\rho_{\parallel}(\sigma), \quad (22)$$

and, then, $\log \rho_1 = \log \rho_{\perp}(\tau) + \log \rho_{\parallel}(\sigma)$.

Let us see how the stream function ψ defined by (21) satisfies the determining equations (15), (17), and (18), i.e., we determine all other fields $I_2(\psi)$, ρ_1 , ρ_2 , ν and h that allow this ψ to be the solution. For arbitrary $f(\tau)$ and $g(\tau)$, we observe

$$\mathcal{L}f = \frac{1}{r^2} [(\tau^2 + 1)f'' + 3\tau f'],$$

$$\nabla f \cdot \nabla g = \frac{1}{r^2}(\tau^2 + 1)f'g'.$$

Hence, the left-hand side of (17) is (denoting $g(\tau) := \log \rho_{\perp}(\tau)$)

$$\mathcal{L}\psi - \nabla\psi \cdot \nabla \log \rho_1 = \frac{1}{r^2} [(\tau^2 + 1)\psi'' + 3\tau\psi' - (\tau^2 + 1)g'\psi']. \quad (23)$$

For this quantity to balance with the right-hand side of (17), $r^{-2}\rho_1$ must be a function of τ if $I_2'(\psi) \neq 0$. Instead of demanding this relation for ρ_1 (cf. Remark 2), we recourse to an assumption $I_2(\psi) = 0$ (the implication of this simple condition will be discussed later). Then, (17) reduces to

$$(\tau^2 + 1)\psi'' + 3\tau\psi' - (\tau^2 + 1)g'\psi' = 0. \quad (24)$$

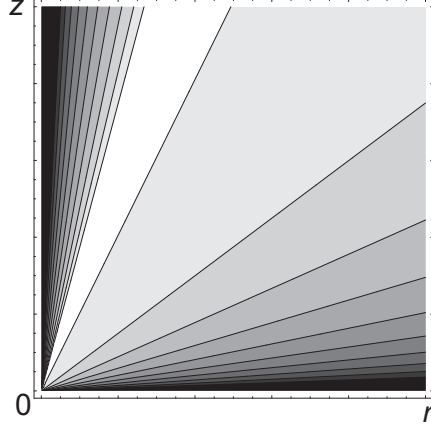


Figure 3. The distribution of ρ_{\perp} of the similarity solution (with $D = 1$, $p = 1$, $J = 0.1$ and $q = 1$). Contour levels are given in the log scale of ρ_{\perp} .

We note that the Beltrami condition (24) is freed from $\rho_{\parallel}(\sigma)$. This fact merits in solving (15); see (27).

For the specific form (21) of ψ , we have to determine an appropriate $g = \log \rho_{\perp}$ to satisfy (24), i.e.,

$$\begin{aligned} g' &= \frac{\psi''}{\psi'} + \frac{3\tau}{\tau^2 + 1} \\ &= \frac{Jp(p-1)\tau^{p+q} + Dq(q+1)}{Jp\tau^{p+q+1} - Dq\tau} + \frac{3\tau}{\tau^2 + 1}. \end{aligned} \quad (25)$$

Solving (25), we obtain

$$g := \log \rho_{\perp} = \log \frac{|Jp\tau^{p+q} - Dq|}{\tau^{q+1}} + \frac{3}{2} \log(\tau^2 + 1),$$

and, thus,

$$\rho_{\perp} = \frac{(\tau^2 + 1)^{3/2} |Jp\tau^{p+q} - Dq|}{\tau^{q+1}}. \quad (26)$$

In Fig. 3, we show the profile of $\rho_{\perp}(\tau)$.

Remark 2 Here we considered the case of $I_2'(\psi) = 0$, but a more general solution can be obtained by demanding $r^{-2}\rho_1$ to be a function of τ . For example, we may put $\rho_1 = \rho_{\perp}(\tau)\rho_{\parallel}(\sigma)$ with $\rho_{\parallel}(\sigma) = \sigma^2 = r^2 + z^2$. Then, $r^{-2}\rho_1 = (1 + \tau^2)\rho_{\perp}(\tau)$.

5.2. Bernoulli relation in the disk region

As mentioned above, this solution assumes $I_2'(\psi) (= \lambda) = 0$, and hence, $I_2 = \rho_2 r V_{\theta}$ must uniformly distribute. In the disk region (the vicinity of $z = 0$), we may approximate $V_{\theta} \approx \sqrt{MG/r}$ (Keplerian velocity). Hence, $\rho_2 \propto r^{-1/2}$. In Fig. 4, we show the profile of $\rho = \rho_1 \rho_2$ for the case of $\rho_1 \propto \rho_{\perp}$ (i.e., $\rho_{\parallel} = \text{constant}$).

For $\rho = \rho_1 \rho_2 = \rho_{\parallel} \rho_{\perp} r^{-1/2}$, (15) reads as

$$\nu \propto \frac{-d\psi/dz}{2\rho_{\parallel}\rho_{\perp}} r^{-3/2} \propto \frac{r^{-5/2}}{\rho_{\parallel}(r)} \quad (27)$$

along each streamline in the disk region. For a given ν , we can solve (27) for ρ_{\parallel} to determine the density profile.

In the disk region the Bernoulli relation (13) accounts as follows: by $\nabla \cdot \mathbf{P} = 0$, we have $P_r = \rho V_r \propto r^{-1}$. If $\rho_{\parallel}(\sigma) = \text{constant}$, for example, $\rho \propto r^{-1/2}$ (evaluated along a streamline in the disk region). Then, we have $V_r = V_{r0} r^{-1/2}$ with a (negative) constant V_{r0} . Combining the azimuthal velocity $V_{\theta} = V_{\theta0} r^{-1/2}$ (which must be slightly smaller than the Keplerian velocity $\sqrt{MG/r}$), we obtain

$$V^2 = (V_{r0}^2 + V_{\theta0}^2)r^{-1} = V_0^2 r^{-1}.$$

By $\rho_2 \propto r^{-1/2}$, we obtain $\partial_r(\log \rho_2) = -(1/2)r^{-1}$. Hence, the Bernoulli relation (13) demands

$$\partial_r h = (V_0^2 - MG)r^{-2},$$

which yields $h = (MG - V_0^2)r^{-1}$. In this estimate, all components of the energy density (gravitational potential ϕ , kinetic energy $V^2/2$ and enthalpy h) have a similar profile ($\propto r^{-1}$).

5.3. Bernoulli relation in the jet region

In the jet region (vicinity of $r = 0$), the streamlines (contours of $\tau = z/r$) are almost vertical, and we may approximate $\sigma \approx z$.

Let us first estimate ρ_2 using (15), which is approximated, in the jet region, by

$$\begin{aligned} r\rho\nu &= \{\log \rho_2, \psi\} \approx (\partial_r \psi) (\partial_z \log \rho_2) \\ &= J p \tau^{p+1} \frac{1}{z} \partial_z (\log \rho_2), \end{aligned} \quad (28)$$

which shows that ρ_2 is an increasing function of $|z|$. Using $\rho = \rho_{\parallel}(\sigma)\rho_{\perp}(\tau)\rho_2$, we integrate (28) along the streamline ($\tau = \text{constant}$, $\sigma \approx z$):

$$\frac{d\rho_2}{\rho_2^2} = -d\left(\frac{1}{\rho_2}\right) = \frac{\nu}{Jp} \tau^{p+2} \rho_{\perp}(\tau)\rho_{\parallel}(z)z^2 dz. \quad (29)$$

With this $\rho_2(z)$, we may estimate the toroidal (azimuthal) component of the velocity: $V_{\theta} = I_2/(r\rho_2) = (I_2\tau)/(z\rho_2)$, where I_2 and τ are constant (the latter is constant along each streamline). We find that the kinetic energy $V_{\theta}^2/2$ of the azimuthal velocity decreases as a function of $|z|$ (both by the geometric expansion factor z^{-2} and the viscosity effect ρ_2^{-2}). The steep gradient of the corresponding hydrodynamic pressure yields a strong boost near the foot point ($z \approx 0$).

The poloidal component of the kinetic energy is estimated as follows: We may approximate

$$\begin{aligned} \frac{1}{2}(V_r^2 + V_z^2) &= \frac{1}{2\rho^2 r^2} |\nabla \psi|^2 \approx \frac{1}{2\rho^2 r^2} \left(J p \frac{z^p}{r^{p+1}} \right)^2 \\ &= \frac{(Jp)^2 \tau^{2p+4}}{2\rho^2 z^4}. \end{aligned} \quad (30)$$

Here, the vertical distribution of the density $\rho = \rho_{\perp}(\tau)\rho_{\parallel}(\sigma)\rho_2$ is primarily dominated by $\rho_{\parallel}(\sigma) \approx \rho_{\parallel}(z)$.

At long distance from the origin, the jet has a natural similarity property. For simplicity, let us ignore the effect of viscosity ($\nu = 0$), and assume $\rho_2 = 1$. Then, $\rho_{\parallel} \propto |z|^{-3/2}$ yields $(V_r^2 + V_z^2)/2 \propto z^{-1}$, which may balance with the gravitational potential energy $\phi = -MG|z|^{-1}$. Note, that the azimuthal component of the kinetic

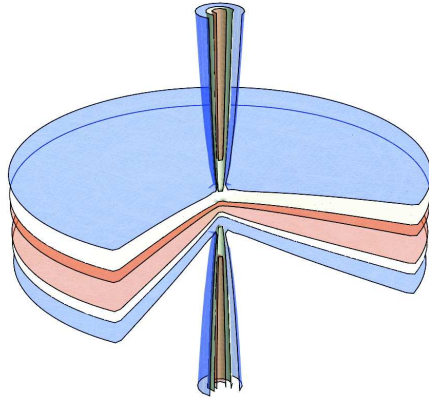


Figure 4. The contours (in log scale) of the density ρ in the similarity solution (21) of the Beltrami model (with parameters $D = 1$, $p = 1$, $J = 0.1$, and $q = 1$).

energy disappears at large scale ($V_\theta^2 \propto z^{-2}$). The Bernoulli condition (13) gives h that also has a similar distribution of $\propto |z|^{-1}$.

Figure 4 shows the profile of $\rho = \rho_\perp \rho_\parallel \rho_2$ with $\rho_\parallel \propto |z|^{-3/2}$ (jet region) and $\rho_2 \propto r^{-1/2}$ (disk region). Dividing \mathbf{P} by the density ρ , we obtain the velocity field \mathbf{V} ; Fig. 1 shows the streamlines of \mathbf{V} corresponding to Figs. 2 and 4.

6. Summary and Concluding Remarks

We have shown that the combination of a thin disk and narrowly-collimated jet is the unique structure that is amenable to the singularity of the Keplerian vorticity; the Beltrami condition—the alignment of flow and *generalized vorticity*—characterizes the geometry. Here the conventional vorticity is generalized as (7) to subtract the viscosity force causing the accretion and the centrifugal force of the Keplerian velocity. Identifying the disk-jet structure as a generalized Beltrami vortex, we will be able to understand the self-organization process in terms of the “generalized helicity.” As we have learned in the present practice, the helicity of the generalized vorticity is the key parameter that characterizes the self-organizing of a disk-jet system.

We end this paper with a short comment on the singularity of the Keplerian velocity. The similarity solution has a singularity at the origin (where $\phi = -MGr^{-1}$ diverges), which disconnects the disk and jet parts of our solution. To “connect” both subsystems, we need a *singular perturbation* that avoids the divergence of physical quantities dictating the small-scale hierarchy on which the disk and jet regions are connected smoothly; Shiraishi *et al.* [22] describes how the different topologies of magnetic field-lines in the disk and jet regions can be connected in a “boundary layer” determined by the the Hall effect in a weakly ionized plasma.

Acknowledgments

The authors are grateful to Professor S. M. Mahajan, Professor R. Matsumoto, Professor G. Bodo, and Professor V. I. Berezhiani for their suggestions and comments. The work of ZY was supported by Grant-in-Aid for Scientific Research (23224014) from MEXT, Japan, and that of NLS was partially supported by the Rustaveli NSF Grant project 1-4/16 (GNSF/ST09-305-4-140).

Appendix A. MHD model

While this article describes a pure fluid-mechanical model of jet collimation, many authors invoke a magnetic field, thrusting the center of the disk, to “guide” (and twist, as often observed) the flow of charged gas (plasma). Here the fluid vorticity plays the same role of a magnetic field. Indeed, the vorticity of the *canonical momentum* combines the fluid vorticity and the magnetic field: $\nabla \times (m\mathbf{V} + q\mathbf{A})$ (m is the mass, q is the charge, and \mathbf{A} is the vector potential of electromagnetic field). Using this “canonical vorticity,” we may readily extend the present model to include the effect of magnetic field (in a Keplerian system, however, the singularity of the fluid vorticity may be the principal part of the canonical vorticity).

The coupling of flow and magnetic field is described by the magnetohydrodynamic (MHD) equations:

$$\partial_t \mathbf{P} + \nabla \cdot (\mathbf{V}\mathbf{P}) = (\nabla \times \mathbf{B}) \times \mathbf{B} - \rho \nabla \phi - \nabla p - \nabla \cdot \mathbf{\Pi}, \quad (\text{A.1})$$

$$\partial_t \mathbf{B} = \nabla \times (\mathbf{V} \times \mathbf{B}), \quad (\text{A.2})$$

where \mathbf{B} is the magnetic field (the magnetic energy density $|\mathbf{B}|^2/8\pi$ is normalized by the kinetic energy density $\mathcal{E}_0 := \rho_0 V_0^2/2$).

A stationary solution of (A.2) is given by

$$\mathbf{B} = \mu \mathbf{P}, \quad (\text{A.3})$$

where μ is a certain scalar function (representing the reciprocal Alfvén Mach number). While (A.3) is not a general solution, other solutions are possible only if the electron pressure p_e or the electrostatic potential φ is huge (of the order of the kinetic energy density \mathcal{E}_0); a perpendicular component of \mathbf{B} with respect to \mathbf{P} causes a Lorentz force on electrons, which must be balanced by a potential force $\nabla(p_e - \varphi)$. If these energy densities are small, \mathbf{B} of order unity is only possible in the parallel direction of \mathbf{P} . Operating divergence on both sides of (A.3), we find $\nabla \cdot (\mu \mathbf{P}) = \mathbf{P} \cdot \nabla \mu = 0$, implying $\mu = \mu(\psi)$.

Adding the magnetic field, the static force balance equation (2) is generalized as

$$\nabla \cdot (\mathbf{V}\mathbf{P}) - [\nabla \times (\mu \mathbf{P})] \times (\mu \mathbf{P}) = -\rho \nabla \phi - \nabla p - \nabla \cdot \mathbf{\Pi}. \quad (\text{A.4})$$

The *generalized vorticity* is now combined with the magnetic field as

$$\widetilde{\mathbf{\Omega}}_2 := \nabla \times \mathbf{P}_2 - \mu \rho_2 \nabla \times \mathbf{B}. \quad (\text{A.5})$$

This generalized vorticity is compared with that of the Hall-MHD theory, i.e. the canonical vorticity [15]. Here the combination of the mechanical and electromagnetic components are scaled by the physical parameters μ (measuring the magnitude of the magnetic field) and ρ_2 (reducing the mechanical component by the viscosity force). The Beltrami equations (16) and (17) are, respectively, generalized as

$$\lambda \rho_1^{-1} \nabla \psi = \nabla (\rho_1^{-1} I) - \mu \rho_2 \nabla (\mu I), \quad (\text{A.6})$$

$$(\rho_1^{-1} - \mu^2 \rho_2) \mathcal{L}\psi + \nabla \psi \cdot (\nabla \rho_1^{-1} - \mu \rho_2 \nabla \mu) = -\lambda \rho_1^{-1} I. \quad (\text{A.7})$$

Combining (A.6) and (A.7), we obtain

$$\mathcal{L}\psi - \nabla\psi \cdot \nabla I = \lambda \frac{|\psi|^2 + I_2 I}{I(1 - \mu^2 \rho)}, \quad (\text{A.8})$$

which reduces into (17) when $\mu = 0$ (i.e. unmagnetized).

References

- [1] BEGELMAN, M. C. 1993 Conference summary. In *Astrophysical Jets* (ed. D. Burgarella et al.), pp. 305–315. Cambridge Univ. Press.
- [2] BLANDFORD, R. D. & PAYNE, D. G. 1982 Hydromagnetic flows from accretion discs and the production of radio jets. *MNRAS* **199**, 883–903.
- [3] CANTARELLA, J., DETRURCK, D., GLUCK, H. & TEYTEL, M. 2000 The spectrum of the curl operator on spherically symmetric domains. *Phys. Plasmas* **7**, 2766–2775.
- [4] CHANDRASEKHAR, S. & KENDALL, P. C. 1957 On force-free magnetic fields. *Astrophys. J.* **126**, 457–460.
- [5] DRITSCHER, D. G. 1991 Generalized helical Beltrami flows in hydrodynamics and magnetohydrodynamics. *J. Fluid Mech.* **222**, 525–541.
- [6] FERRARI, A. 1998 Modeling extragalactic jets. *Annu. Rev. Astron. Astrophys.* **36**, 539–598.
- [7] GONZÁLEZ, R., SARASUA, G. & COSTA, A. 2008 Kelvin waves with helical Beltrami flow structure. *Phys. Fluids* **20**, 024106 1–7.
- [8] HEYVAERTS, J. & PRIEST, E. R. 1984 Coronal heating by reconnection in DC current systems.: a theory based on Taylor’s hypothesis. *Astron. Astrophys.* **137**, 63–78.
- [9] ITO, N. & YOSHIDA, Z. 1996 Statistical mechanics of magnetohydrodynamics. *Phys. Rev. E* **53**, 5200–5206.
- [10] KAMPEN, N. G. VAN & FELDERHOF, B. U. 1967 *Theoretical Methods in Plasma Physics*, Chap. 5. North-Holland.
- [11] KUSANO, K., SUZUKI, Y. & NISHIKAWA, K. 1995 A solar flare triggering mechanism based on the Woltjer-Taylor minimum energy principle. *Astrophys. J.* **441**, 942–951.
- [12] LIVIO, M. 1997 The formation of astrophysical jets. in *Accretion Phenomena and Related Outflows, IAU Colloquium 163* (ed. D. T. Wickramasinghe, et al.), pp. 845–866. ASP.
- [13] LIVIO, M. 1999 Astrophysical jets: a phenomenological examination of acceleration and collimation. *Phys. Rep.* **311**, 225–245.
- [14] LOW, B. C. 1982 Nonlinear force-free magnetic fields. *Rev. Geophys. Space Phys.* **20**, 145–159.
- [15] MAHAJAN, S. M., & YOSHIDA, Z. 1998 Double curl Beltrami flow —diamagnetic structures. *Phys. Rev. Lett.* **81**, 4863–4866.
- [16] MAHAJAN, S. M., NIKOL’SKAYA, K. I., SHATASHVILI, N. L. & YOSHIDA, Z. 2002 Generation of flows in the solar atmosphere due to magnetofluid coupling. *Astrophys. J.* **576**, L161–164.
- [17] MOFFATT, H. K. 1978 *Magnetic field generation in electrically conducting fluids*. Cambridge Univ. Press.
- [18] MORRISON P. J. 1998 Hamiltonian description of the ideal fluid. *Rev. Mod. Phys.* **70**, 467–521.
- [19] OHSAKI, S., SHATASHVILI, N. L., YOSHIDA, Z., & MAHAJAN, S. M. 2001 Magnetofluid coupling: eruptive events in the solar corona. *Astrophys. J.* **559**, L61–L65.
- [20] SHAN, X., MONTGOMERY, D. & CHEN, H. 1991 Nonlinear magnetohydrodynamics by Galerkin-method computation. *Phys. Rev. A* **44**, 6800–6818.
- [21] SHATASHVILI, N. L. & YOSHIDA, Z. 2011 Generalized Beltrami field modeling disk-jet system. *AIP Conf. Proc.* **1392**, 73–82.
- [22] SHIRAIISHI, J., YOSHIDA, Z., & FURUKAWA, M. 2009 Topological transition from accretion to ejection in a disk-jet system —singular perturbation of the hall effect in a weakly ionized plasma. *Astrophys. J.* **697**, 100–105.
- [23] SUDAN, R. N. 1979 Stability of field-reversed, force-free, plasma equilibria with mass flow. *Phys. Rev. Lett.* **42**, 1277–1281.
- [24] TANG, X. Z. 2011 Numerical computation of the helical Chandrasekhar-Kendall modes. *J. Comp. Phys.* **230**, 907–919.
- [25] TAYLOR, J. B. 1974 Relaxation of toroidal plasma and generation of reverse magnetic fields. *Phys. Rev. Lett.* **33**, 1139–1141.
- [26] TAYLOR, J. B. 1986 Relaxation and magnetic reconnection in plasmas. *Rev. Mod. Phys.* **58**, 741–763.
- [27] WOLTJER, L. 1958 A theorem on force-free magnetic fields. *Proc. Natl. Acad. Sci. U. S. A.* **44**, 489–491.

- [28] YANG, Y.-T., SU, W.-D. & WU, J.-Z. 2010 Helical-wave decomposition and applications to channel turbulence with streamwise rotation. *J. Fluid Mech.* **662**, 91–122.
- [29] YOSHIDA, Z. & GIGA, Y. 1990 Remarks on spectra of operator rot. *Math. Z.* **204**, 235–245.
- [30] YOSHIDA, Z. 1991 Helicity waves propagating in plasma. *J. Plasma Phys.* **45**, 481–488.
- [31] YOSHIDA, Z., OHSAKI, S., ITO, A. & MAHAJAN, S. M. 2003 Stability of Beltrami flows. *J. Math. Phys.* **44**, 2168–2178.
- [32] YOSHIDA, Z., MAHAJAN, S. M., MIZUSHIMA, T., YANO, Y., SAITOH, H. & MORIKAWA, J 2010 Generalized two-fluid equilibria —Understanding RT-1 experiments and beyond. *Phys. Plasmas* **17**, 112507 1-7.
- [33] YOSHIDA, Z. 2011 Nonlinear Alfvén/Beltrami waves —an integrable structure built around the Casimir. *Comm. Nonlinear Sci. Num. Sim.* **17**, 2223-2232.